JOURNAL OF Applied Polymer SCIENCE

Lignocellulosic Byproducts as Filler in Polypropylene: Comprehensive Study on the Effects of Compatibilization and Loading

Michael A. Fuqua, Venkata S. Chevali, Chad A. Ulven
Mechanical Engineering Department, North Dakota State University, Fargo, North Dakota 58108

Correspondence to: C. A. Ulven (E-mail: chad.ulven@ndsu.edu)

ABSTRACT: Lignocellulosic byproducts derived from biofuel processes were analyzed as functional fillers in polypropylene-based biocomposites. Corn cob, a byproduct yielded from corn harvesting for ethanol production, and sunflower hull, a byproduct of seed stripping for biodiesel production, were both examined as ground filler agents. Composite blends with these lignocellulosic fillers at four filler loadings and four variants of surface compatibilizer loading were melt-compounded using a twin screw extruder and injection molded into test specimens. Tensile testing, notched Izod impact testing, and thermal-mechanical analysis were performed on the composites. The role of filler type, loading, and surface compatibilization were established and reported. Additionally, elastic modulus and tensile strength were successfully modeled using established particulate composite models. © 2012 Wiley Periodicals, Inc. J. Appl. Polym. Sci. 000: 000–000, 2012

KEYWORDS: fillers; compatibilization; polypropylene; mechanical properties

Received 5 November 2010; accepted 29 March 2012; published online
DOI: 10.1002/app.37820

INTRODUCTION

The widespread use of plastics has brought about modifications of these systems with functional fillers. Through the addition of fibers and particulates, alterations and improvements can be made to the properties of base plastics, often times at low cost, while subsequently reducing the net polymer usage of a given material. Inorganic fillers such as layered talc, mica, nanoclays, kaolin, wollastonite, and $CaCO_3$ have thus seen acceptance into the polymer molding industry.[1] These fillers have demonstrated a variety of property modifications to base polymers, including improvements in strength, stiffness, thermal stability, melt viscosity, impact, and conductivity.

Another approach in functional filler development has been into the use of organic lignocellulosic materials. These fillers are built around a backbone of cellulose, a crystalline straight chain. The cellulose polymer contains numerous hydroxyl groups, and these hydroxyl groups are capable of forming hydrogen bonds with the oxygen molecules of other cellulose chains. This produces cellulose microfibrils, which have excellent strength and stiffness properties due to the hydrogen bonding, allowing them to reinforce the lignocellulosic material.

At present, the focal point of lignocellulosic filler research has been into the development of wood–plastic composites filled with wood fibers or wood flour. Commercially, wood–plastic composites are used mainly as a composite lumber material, finding applications in decking, fencing, and moldings and trim, among others. This commercial focus has placed reliance upon the ability of wood flour to yield more rigid plastics when incorporated at higher loadings. To this end, the utilization of these fillers within polymers such as polypropylene (PP) has been extremely successful. At 40 wt % wood flour loading, researchers have reported increased modulus values over neat PP by 130% to 180%.[2,3]

The hydrophobic nature of polyolefins such as PP is an issue when attempting to create blends with lignocellulosic fillers, which are inherently hydrophilic. The low polar affinity between the hydrophilic filler and hydrophobic matrix restricts proper interaction between these two constituents, leading to decreases in strength when untreated wood flour is added. To alleviate this obstacle, chemical compatibilizers such as maleic anhydride grafted PP (MAPP) have been developed. MAPP alters the surface of the hydrophilic cellulose fiber, altering the surface creating a hydrophobic interface with the polymer chains of the matrix.[4,5] This change in matrix–filler interface has resulted in wood–plastic composites with strength performances that are nearly equivalent to that of unfilled PP, even at high filler loading levels.[2,3,6]

However, wood fibers and flour are not the only lignocellulosic materials being examined for use as functional fillers in thermoplastics. Rice husk flour,[7] wheat husk, rye husk,[8] wheat straw,[9] and sugarcane bagasse[10] have all been examined with different degrees of success. With an abundance of these materials being yielded with little commercial value, addressing their potential as functional fillers serves a strong purpose.

Increasingly in the last decade, expansion seen in the biofuel sector has managed to dramatically change the dynamic of the United States' agricultural market. Crops traditionally grown as food have found a lucrative market as biofuel feedstock. These maturing industries have brought with them new sources of lignocellulosic material in the form of biofuel production byproducts. The objective of this research was to investigate the performance of alternative lignocellulosic byproducts derived from biofuel byproducts as functional fillers in PP. In this study, focus was placed on two particular fillers, corn cob and sunflower hull. Both were chosen due to the potential they have demonstrated as functional fillers in previous exploratory studies.[11-13] In this work, a more comprehensive understanding of how the two fillers perform at various loading levels with variation in MAPP compatibilizer is examined.

EXPERIMENTAL

Materials

Two sources of lignocellulosic filler were explored in this work. The first was ground sunflower hull, supplied by Red River Commodities, Inc., USA (Fargo, ND), and the second was ground corn cob, supplied by Best Cob, LLC (Independence, IA). Both fillers were fractionated to a maximum size of 250 μm. The major chemical constituents of the two lignocellulosic fillers, as compared with soft wood[8] used in wood–plastic composites, are provided in Table I.

The base-polymer chosen for this study was a homopolymer PP, with a density of 0.905 g/cm^3 and melt flow rate of 30 g/10 min, supplied by Total Petrochemicals, USA, under the trade name TOTAL Polypropylene 3825. The surface compatibilizer used in this study was an MAPP, trade name Licomont AR 504 by Clariant, with a 3.5 wt % maleic anhydride level and a density of 0.910 g/cm^3.

Composite blends of 10, 20, 30, and 40 wt % filler were explored for both the sunflower hull and corn cob. Correspondingly, MAPP was used as a compatibilizer at MAPP to filler ratios of 0 : 1, 1 : 20, 1 : 10, 1 : 5, and 2 : 5 for all filler loadings. This resulted in a comprehensive test matrix, neglecting a virgin PP control, of 20 composite blends for each the sunflower hull and corn cob fillers, resulting in 40 composite blends being examined. Designation used will be 'PP-X-YY-ZZ', where X is representative of the filler type (either S for sunflower hull or C for corn cob), YY is the wt % of filler loaded, and ZZ is the percentage MAPP to filler.

Composite Preparation

The PP, MAPP, and lignocellulosic fillers explored in this study were melt blended using an 18 mm apparent diameter lab scale co-rotating twin screw extruder (Leistritz Micro-18/GL-40D) to yield composite blends. The screw rotation rate was set at 350 rpm and the temperature profile from hopper to die was 149°C, 182°C, 185°C, 189°C, 195°C, 195°C, and 195°C. The extruded strands were quenched in a water bath, air dried, and then pelletized. The pelletized composite blends were subsequently dried for 12 h at 80°C. The dried composite pellets were then injection molded into final test specimens using a 50 ton Technoplas, Inc., SIM 5080 injection molder. The temperature profile from hopper to nozzle tip was 193°C, 199°C, 204°C, 210°C, and 204°C.

Table I. Lignocellulosic Filler Constituent Content

Dry mass (%)	Sunflower hull	Corn Cob	Soft wood[2]
Cellulose	46.0	33.0	42.0
Hemicellulose	17.0	37.0	22.0
Lignin	19.0	5.0	31.0
Starch	1.5	6.0	0.5
Ash	2.5	3.5	-
Protein	4.5	2.5	0.5

Characterization

Tensile mechanical testing was performed in displacement control at a rate of 5 mm/min, according to ASTM standard D-638 using an Instron model 5567 load frame. Notched Izod impact testing was performed using off standard dimensioned specimens (3.9 mm × 9.8 mm), following ASTM standard D-256 as a procedural guide using a Tinius Olson IT 504 Izod testing frame with an Impact 104 controller. The coefficient of linear thermal expansion (CTE) was found by thermal mechanical analysis using a TA Q800 DMA in static mode. A tensile fixture was used, operated at a controlled 0 N force maintained for a 5°C/min temperature ramp from ambient to 125°C. The CTE is calculated by the following:

$$\alpha = \frac{1}{L_0}\frac{\partial L}{\partial T} \quad (1)$$

where α is the CTE, L_0 is the initial length of a specimen, L is the new length, and T is the temperature.

RESULTS AND DISCUSSION

Table II shows the obtained tensile, impact, and thermal expansion properties of the sunflower hull and corn cob-filled PP specimens produced in this study. The effects of filler loading and utilization of MAPP as a compatibilizer were examined as functions of the averaged effects of either variable for each property. In this manner, trends are observed which indicate the effectiveness of material variation upon property variation.

Tensile Properties

Tensile Strength. Tensile strength analysis demonstrates that optimizing the compatibilizer usage to achieve optimal polarity matching between filler surface and matrix, without contributing to the overall weakening of the composite, is critical. Figure 1 presents an averaged role MAPP loading on tensile composite performance, independent of filler loading amount. For both sunflower hull and corn cob filler, it is found that the utilization of MAPP at any loading level is preferential to no compatibilizer

Table II. Resultant Properties of Full-Scale Study with Corresponding SD

	Tensile strength (MPa)	SD	Elastic modulus (MPa)	SD	Elongation to failure (%)	SD	Notched Izod impact (J/m^2)	SD	CTE ($\times 10^{-6}$/°C)	SD
PP	30.00	0.25	1737.90	57.60	350.00	-	2160.13	196.84	2.66	0.07
PP-S-10-00	27.38	0.22	2142.91	46.08	16.40	3.50	2435.63	293.88	2.51	0.01
PP-S-10-05	29.09	0.13	2049.03	155.53	14.30	1.60	1962.12	50.73	2.32	0.03
PP-S-10-10	29.28	0.16	2145.83	120.14	13.50	1.10	2140.90	186.52	2.36	0.02
PP-S-10-20	29.34	0.21	2009.81	28.49	13.00	0.90	2307.20	354.96	2.51	0.01
PP-S-10-40	28.90	0.16	2067.49	79.62	11.80	1.20	2249.88	274.81	2.37	0.05
PP-S-20-00	26.04	0.12	2458.08	72.78	12.30	1.00	1943.04	198.20	1.92	0.03
PP-S-20-05	29.05	0.21	2478.91	96.95	10.30	0.40	2144.59	117.05	1.96	0.10
PP-S-20-10	29.83	0.16	2716.17	71.07	9.10	1.00	2080.00	74.17	1.91	0.01
PP-S-20-20	28.90	0.16	2535.69	117.07	9.50	0.20	1991.46	43.66	1.97	0.01
PP-S-20-40	27.26	0.17	2448.12	111.33	9.20	0.70	1990.05	70.10	1.97	0.07
PP-S-30-00	25.63	0.35	2922.10	95.80	4.50	0.80	2029.00	107.45	1.42	0.06
PP-S-30-05	29.49	0.12	2792.70	79.90	3.30	0.50	1948.59	208.07	1.42	0.02
PP-S-30-10	28.72	0.23	2583.60	165.80	3.60	0.70	1676.08	66.66	1.30	0.01
PP-S-30-20	28.38	0.26	2532.90	144.60	3.10	0.50	1951.51	92.36	1.30	0.03
PP-S-30-40	27.00	0.32	2608.70	58.40	2.90	0.40	1902.39	290.16	1.42	0.02
PP-S-40-00	22.90	0.28	3072.60	248.80	4.20	0.90	2084.36	109.62	1.02	0.04
PP-S-40-05	30.23	0.20	3122.20	173.70	2.50	0.40	1661.32	136.99	1.08	0.01
PP-S-40-10	30.12	0.37	3157.30	197.60	2.20	0.40	1776.73	71.05	1.06	0.00
PP-S-40-20	29.27	0.36	3384.80	273.10	1.80	0.20	1693.48	225.07	1.07	0.01
PP-S-40-40	24.82	0.57	3274.10	145.80	1.20	0.10	1275.12	58.10	1.06	0.10
PP-C-10-00	27.42	0.22	2085.60	149.40	11.40	3.00	2761.61	221.29	2.87	0.07
PP-C-10-05	29.31	0.13	2165.00	78.80	9.20	1.40	2180.42	228.59	2.82	0.03
PP-C-10-10	29.30	0.13	2032.80	61.30	10.70	2.60	2298.58	255.36	2.68	0.07
PP-C-10-20	29.56	0.17	2152.50	133.70	12.00	1.90	2210.89	250.83	2.69	0.02
PP-C-10-40	29.14	0.08	2131.20	130.90	10.30	0.90	2136.20	274.23	2.77	0.02
PP-C-20-00	23.42	0.09	2338.36	72.73	13.00	0.90	2471.36	256.76	2.28	0.06
PP-C-20-05	28.49	0.24	2375.20	45.20	4.90	0.40	2247.80	247.77	2.39	0.10
PP-C-20-10	26.94	0.11	2366.16	87.26	8.70	0.80	1995.44	110.77	2.36	0.06
PP-C-20-20	28.30	0.22	2379.00	138.90	5.00	1.00	1913.84	246.50	2.45	0.01
PP-C-20-40	27.95	0.24	2381.20	106.00	4.40	0.60	1863.15	85.83	2.42	0.06
PP-C-30-00	22.47	0.18	2596.90	151.30	5.60	0.80	1927.31	186.73	2.04	0.07
PP-C-30-05	27.06	0.54	2641.50	240.90	2.90	0.40	1935.28	101.67	2.07	0.04
PP-C-30-10	28.63	0.40	2667.10	129.90	2.90	0.50	2022.69	83.46	2.17	0.00
PP-C-30-20	28.56	0.26	2806.60	298.40	3.20	0.50	1895.68	101.58	2.15	0.05
PP-C-30-40	26.72	0.56	2643.20	155.80	2.30	0.30	1947.35	208.39	2.12	0.07
PP-C-40-00	18.58	0.23	2489.90	212.70	3.90	0.50	1886.77	185.22	1.54	0.09
PP-C-40-05	27.66	0.09	2825.10	170.50	2.00	0.40	1898.71	135.10	1.60	0.01
PP-C-40-10	28.15	0.27	2810.80	204.70	1.90	0.30	1935.86	17.16	1.92	0.03
PP-C-40-20	27.06	0.32	2634.30	115.00	1.70	0.10	1297.06	232.08	1.89	0.04
PP-C-40-40	23.46	0.60	2648.80	52.90	1.20	0.10	1031.28	227.85	1.83	0.17

usage in retaining strength in the blends. The inherent polarity differences between the lignocellulosic fibers and PP leads to limited chemical interaction and surface void formation when no compatibilizer is used. Without a proper interfacial bond, the fillers are not able to be used as effective mechanical reinforcement. However, through the utilization of low amounts of MAPP as a compatibilizer, a bridge can be made between the hydrophilic fibers and hydrophobic matrix system, which leads to significant improvements in strength.[14,15]

Applied Polymer SCIENCE

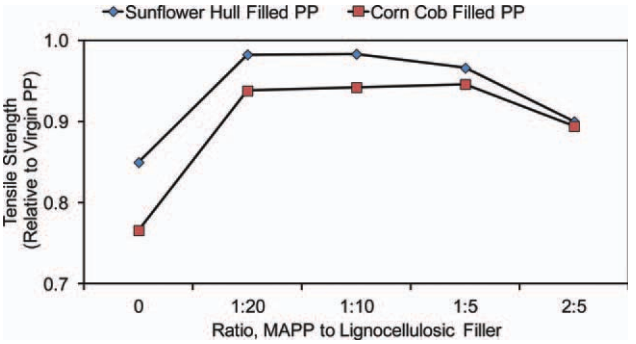

Figure 1. Relative tensile strength of PP composites as a function of MAPP to filler ratio, normalized across all filler loading concentrations. [Color figure can be viewed in the online issue, which is available at wileyonlinelibrary.com.]

It is found that the lowest ratio of compatiblizer to filler studied was adequate to achieve optimal strength properties. Doubling the compatibilier to filler ratio from 1 : 20 to 1 : 10 shows little change in strength, indicating that while level of cellulose to maleic anhydride may be increased, the level of potential additional surface interaction improvement. This is further confirmed by noting that the cellulose difference in the two filler yielded only minor differences in strength trends at these low compatibilizer loadings. However, it is also observed that excessive MAPP loading can be detrimental, as a 2 : 5 MAPP to filler ratio sees significant decreases in strength versus lower MAPP loadings. The low molecular weight of the MAPP allows for the interaction between the PP matrix and the MAPP to become dominated principally by van der Waals forces, because chain entanglement is nearly impossible.[16] Loop conformations are maintained by the anhydride units of the MAPP within the blends due to the compatibilizer being able to act with equal probability with the cellulose in the lignocellulosic fillers. As such, any excess MAPP not coupled together with cellulose to help the interfacial interaction with the matrix is left to contribute to decreases in the composite's strength.

The strength performance of the fillers blended into PP can be expressed quantitatively using a simple model which relates the strength of the blended particulate composite, σ_c at a filler volume fraction, V_p, to the unfilled PP strength, σ_m, through a hyperbolic function[17]:

$$\sigma_c = \left[\frac{1 - V_p}{1 + 2.5V_p}\sigma_m\right]\exp(BV_p) \tag{2}$$

where B is a constant empirically derived relating to surface area, particle density, and interfacial bonding energy, which effectively expresses the load bearing capacity of the filler within the composite. While not directly tied to any physical meaning, this interfacial parameter has been found to loosely correlate, beyond adhesion, to specific surface area, as smaller particles with good interfacial bonding have shown to be fitted using higher values of B. Because of the low degree of elongation observed in the particulate filled composites, B can be found as the slope of straight line fitted to ln σ_{red} plotted against filler content,[18] where:

$$ln\sigma_{red} = ln\sigma_c \frac{1 + 2.5V_p}{1 - V_p} = ln\sigma_m + BV_p \tag{3}$$

Using eq. (3), specific values of B can be determined for both corn cob and sunflower fillers with and without MAPP addition acting as compatibilizer. For these fits, the density measurements of the resultant composite blends are used to determine the filler volume fraction of lignocellulosic material in the PP blends.

Attention was placed on two distinct trends in the lignocellulosic filled systems, one in which no modifier is used and thus poor interfacial adhesion is achieved, and a second in which an ideal MAPP to filler ratio is utilized to obtain optimal interfacial adhesion. The curve fits achieved through this fitting, as shown in Figure 2, are able to not only accurately address interfacial adhesion effects, but also differences within the two filler's mechanical capabilities due to constituent makeup. Sunflower hull, having a slightly larger crystalline cellulose concentration compared with the corn cob filler, expectantly performs slightly better both with and without an MAPP compatibilizer.

Elastic Modulus. Analysis of the normalized effects of MAPP loading upon the elastic modulus performance of the lignocellulosic particulate filled composites is found to show that compatibilizer usage does not play a significant role upon the modulus performance (Figure 3). Modulus enhancement is the result of the fillers exerting a resistance against the plastic deformation of the PP matrix, which restricts polymer chain elongation. The MAPP used in this study has a relatively low molecular weight, and thus does not produce significant chain entanglement within the matrix. This in turn prevents it from leading to additional increases in elastic modulus compared with the use of untreated filler.

Although there is a small degree of variation, overall the two filler types produce very similar increases in elastic modulus with

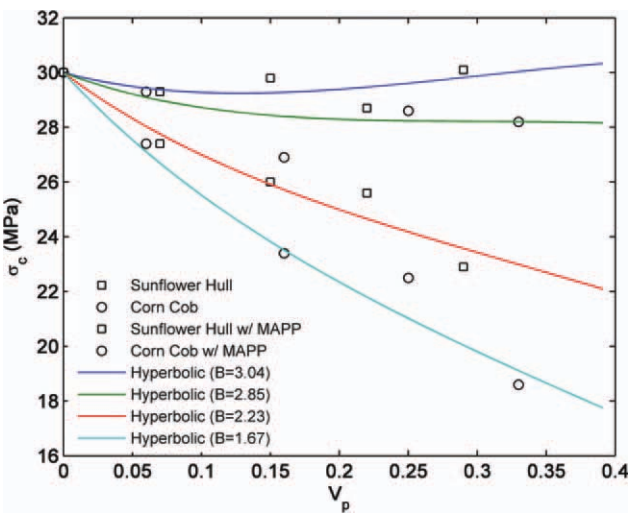

Figure 2. Hyperbolic model fits to strength performance of corn cob and sunflower hull filled PP with and without proper compatibilization. [Color figure can be viewed in the online issue, which is available at wileyonlinelibrary.com.]

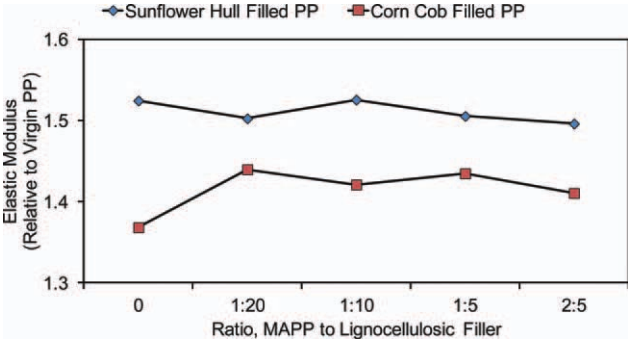

Figure 3. Relative elastic modulus of PP composites as a function of MAPP to filler ratio, normalized across all filler loading concentrations. [Color figure can be viewed in the online issue, which is available at wileyonlinelibrary.com.]

increased filler loading. This allows for the application of single phase algorithmic modulus fits to relate the effect of filler loading on stiffness. As has been demonstrated in wood–flour filled thermoplastic composite systems,[19] it has been possible to relate other lignocellulosic filled composite systems to Einstein's relationship. By assuming a perfect distribution of filler and perfect adhesion between particulates and matrix, Einstein's equation predicts the composite modulus, E_c, as a linear relationship between particulate loading and matrix elastic modulus, E_m[20,21]:

$$E_c = E_m(1 + 2.5V_p) \tag{4}$$

However, due to the inability for this method to account for strain field interactions around particles, the low concentration requirement causes it to underpredict modulus values as filler loading is increased. This trend is observed when fitted against the corn cob and sunflower hull filled PP composites in this study Figure 4. Although it does show a close linear fit to the data, it slightly underpredicts performance for the sunflower hull, a problem which is believed would be exacerbated with greater filler loading.

An alternative single phase model, proposed by Kerner,[22] calculates the composite modulus based on particulate loading, considering both matrix modulus and Poisson's ratio, v_m. In this model, spherical particles are assumed to be distributed randomly throughout the given matrix, so that gross isotropy is always applicable and restriction upon particulate size is not necessary. The derivation is done through the construction of an average grain surrounded by an average shell of suspending medium, further surrounded by an average medium of the matrix, yielding the following:

$$E_c = E_m\left(1 + \frac{V_p}{V_m}\frac{15(1 - v_m)}{8 - 10v_m}\right) \tag{5}$$

By assuming $v_m = 0.3$, another representation of the effects of filler loading upon modulus can be made, as shown in Figure 4. However, at higher filler loadings Kerner's model increases at a greater rate than at small loadings, and as such may not accurately model the effects of filler loading at higher concentrations than those studied in this work.

To address the discrepancies found in the application of Einstein and Kerner's single phase models at higher filler loadings, it is possible to apply a two phase model, in which a modulus is assumed for the lignocellulosic particulates. Fitting the model with an assumed filler modulus of $E_p = 18$GPa a two-phase model proposed by Counto[23] can be examined which is shown to follow the data fairly well.

$$\frac{1}{E_c} = \frac{1 - \sqrt{V_p}}{E_m} + \frac{1}{(1 - \sqrt{V_p})/(\sqrt{V_p}E_m) + E_p} \tag{6}$$

Counto's approach models blends as an encompassed prism particulate centered in a prism of matrix, assuming perfect bonding between filler and matrix. The main assumption is that as E_p decreases, the elastic strain, as well as strains related to creep and creep recovery of the matrix increase in relation to the volume concentration of particulate. This model has the benefit of fitting the lignocellulosic data through higher filler concentrations, but loses applicability as loading approaches zero.

Elongation to Failure. The addition of lignocellulosic filler at any loading degree will overall have a lessening effect upon the elognation to failure of the PP system. The unfilled PP has a high degree of elongation (>350%) due to its ability to achieve chain alignment and high degrees of necking without restriction during plastic deformation. In comparison, the addition of the lignocellulosic filler restricts the mobility and deformability of the PP matrix, leading to failure initiation soon into the plastic regime. As is shown in Figure 5, the addition of filler at higher loadings tends to cause failure to occur earlier than at lower loadings. By 40 wt % filler addition, failure was observed to occur soon after ultimate tensile strength is reached. It is believed that additional filler loading would decrease the degree of elongation to failure only due to increased stiffness of the

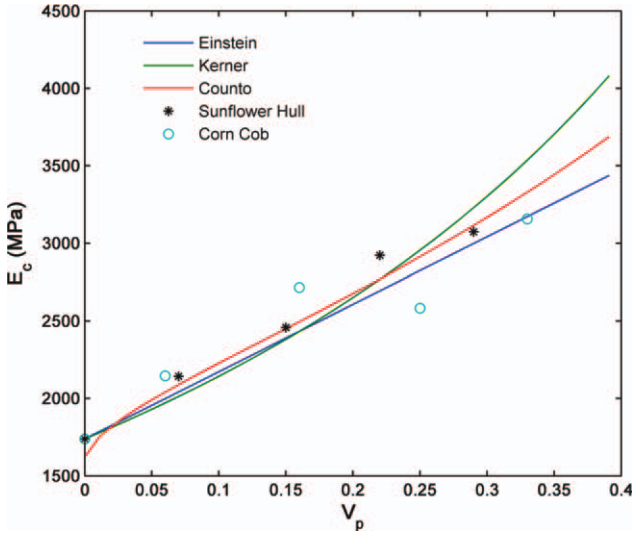

Figure 4. Elastic modulus model fits for corn cob and sunflower hull filled PP. [Color figure can be viewed in the online issue, which is available at wileyonlinelibrary.com.]

Applied Polymer SCIENCE

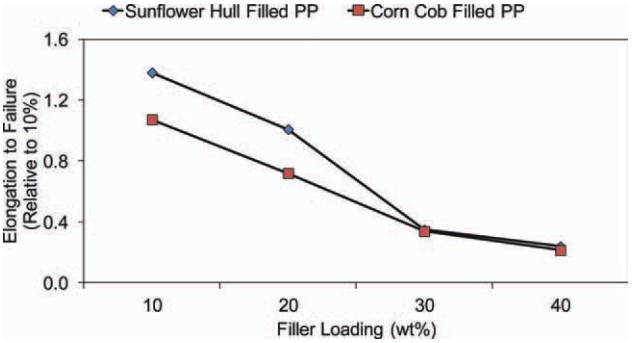

Figure 5. Averaged effect of filler loading upon the ultimate elongation to failure of the PP blends. [Color figure can be viewed in the online issue, which is available at wileyonlinelibrary.com.]

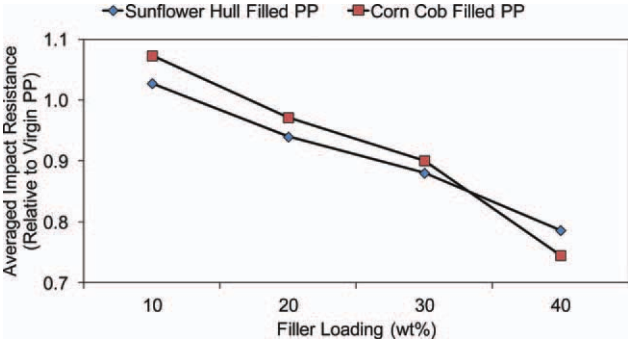

Figure 7. Averaged effect of filler loading upon the notched Izod impact resistance of the PP blends. [Color figure can be viewed in the online issue, which is available at wileyonlinelibrary.com.]

material, rather than through any change in the degree of plastic deformation after ultimate stress.

A decrease in elongation to failure is also observed due to the utilization of MAPP as a compatibilizer, as shown in Figure 6. As MAPP concentration is increased, more free chains from the compatibilizer are introduced into the matrix. Because of the inability for these chains to entangle with the polymer matrix, smaller deformation is introduced at the interphase between filler and matrix, leading to reduced elongation to failure.[6] To maximize elongation to failure while using a compatiblizer, it is thus advisable to maintain as low of a compatilizer use as possible while ensuring strength requirements are met.

Impact

The results of the averaged effect of sunflower hull and corn cob addition on the notched Izod impact performance of PP composite blends are shown in Figure 7. As the filler content is increased, a decrease in the impact performance is observed. This is due to the filler providing points of stress concentration within the PP matrix, which allows for crack propagation to occur more readily than in a virgin matrix. As filler content is increased, these points of stress concentration are increased, and crack growth along the relatively weak interphase between particulates and matrix is more easily propagated.

Because the stress concentrations around the particles leading to crack propagation and subsequent failure upon the impact load are responsible for the decrease in impact resistance observed through the notched Izod testing, it would be speculated that the use of MAPP as a compatibilizer would cause an increase in impact performance in comparison. Yet it is observed in Figure 8 that when the averaged effect of MAPP addition is examined, the result is unanimously detrimental to impact resistance. While a proper MAPP to filler loading ratio increases interfacial adhesion, the low molecular weight system also is incapable of forming entanglements with the PP matrix, which subsequently allows for easier crack propagation, and thus lowered impact performance.[3] Thus, while MAPP is shown to be necessary for strength improvement, it is demonstrated that maintaining as low of a compatilizer use as possible while maintaining strength requirements is advisable when considering impact performance.

CTE

A major limitation to the use of plastics in many applications is their large degree of dimensional variation with thermal changes. Maintaining dimensional tolerances when large thermal cycles are experienced, such as in outdoor applications, is difficult in products produced from unreinforced plastics. However, the addition of fillers such as the lignocellulosic byproducts examined in this study can assist in improving the thermal dimensional stability by restricting polymer chain movement during thermal changes.

It was found that the MAPP loading did not play any significant role upon CTE performance with filler loading of PP, and

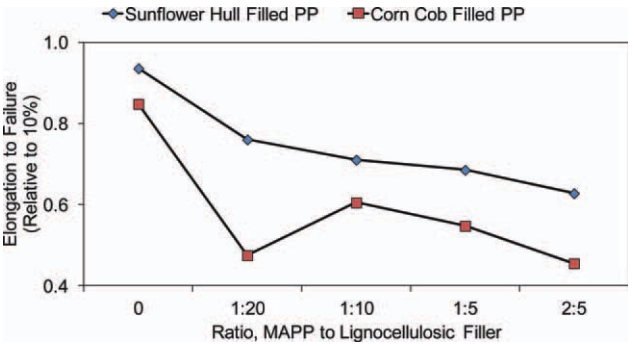

Figure 6. Averaged effect of MAPP loading upon the ultimate elongation to failure of the PP blends. [Color figure can be viewed in the online issue, which is available at wileyonlinelibrary.com.]

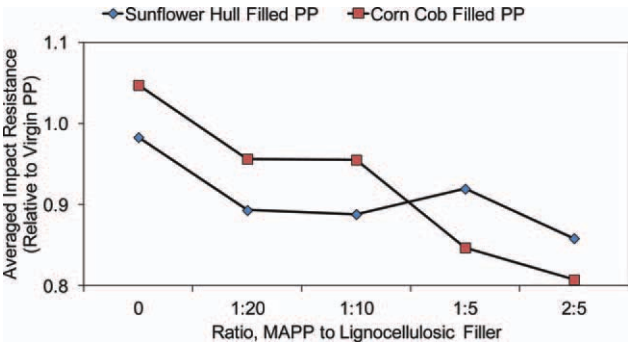

Figure 8. Averaged effect of MAPP loading upon the notched Izod impact resistance of the PP blends. [Color figure can be viewed in the online issue, which is available at wileyonlinelibrary.com.]

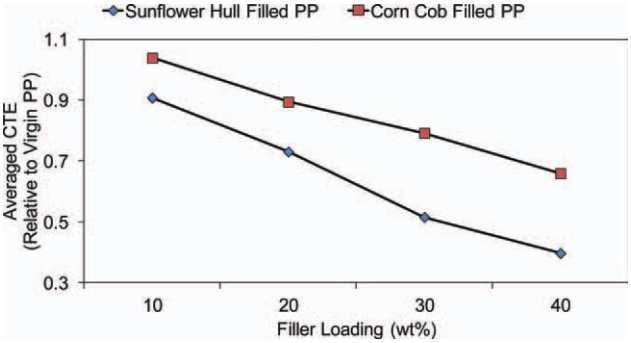

Figure 9. Averaged effect of filler loading upon the coefficient of thermal expansion of the PP blends. [Color figure can be viewed in the online issue, which is available at wileyonlinelibrary.com.]

as such, an analysis of filler effect upon thermal dimensional stability can be limited to an averaged effect of filler loading. It is observed in the normalized results found in Figure 9 that the addition of lignocellulosic filler results in a reduction in the dimensional change of PP. As filler loading is increased, both sunflower hull and corn cob filler addition lead to a restriction in the polymer chain movement of the matrix, resulting in relatively linear decreases in CTE in comparison with loading level. Because lowering of CTE is dependent on increased bond energies, which are highest within the cellulose constituent of the lignocellulosic fibers, cellulose serves as the greatest potential agent in lignocellulosic materials for lowering the CTE of a polymer blend. This explains why the ground sunflower hull showed larger decreases in CTE versus an equivalent weight loading of the ground corn cob.

CONCLUSIONS

This study examined the potential of using corn cob and sunflower hull lignocellulosic byproducts as functional fillers in PP. The following conclusions can be drawn:

- Through the proper utilization of a compatibilizer such as MAPP, strength comparable with virgin PP can be achieved. It was found that a low ratio, 1 : 20 compatibilizer to filler (% w/w) was subsequent to achieve optimal results. This level is not necessarily an optimal point, and lower ratios could potentially reveal that compatibilizer loading can be further reduced without sacrificing the strength gains obtained through compatibilizer use.
- The amount of cellulose present in the fillers plays a small role in tensile strength. With and without proper surface interaction with the matrix, sunflower hull slightly outperformed corn cob. These changes were capable of being modeled using a hyperbolic model.
- Elastic modulus increased independent of compatibilizer loading, and was found to be similar for both corn cob and sunflower hull. This can be predicted using established particulate models from Kerner, Counto, and Einstein.
- The addition of filler lead to significant decreases in the elongation to failure of the composite blends in comparison with unfilled PP. Increased filler loading lead to greater brittleness, as did increased compatibilizer usage.
- The impact performance was slightly lowered with the addition of both corn cob and sunflower hull. Compatibilizer usage did not positively improve impact performance.
- The coefficient of thermal expansion decreased with increased addition of both fillers, without compatibilizer playing a major role. The higher cellulose content sunflower hull saw greater decreases in expansion.

ACKNOWLEDGMENTS

The authors gratefully acknowledge the funding support provided by the North Dakota Corn Utilization Council and the SUNRISE BioProducts Center of Excellence. The authors acknowledge the material donations of MCG Biocomposites, LLC, and Red River Commodities, Inc.

REFERENCES

1. Xanthos, M., Ed. Functional Fillers for Plastics; Wiley-VCH: Weinheim, **2005.**
2. Anglès, M. N.; Salvadó, J.; Dufresne, A. Steam-exploded residual softwood-filled polypropylene composites. *J. Appl. Polym. Sci.* **1999,** *74*, 1962.
3. Dányádi, L.; Renner, K.; Szabó, Z.; Nagy, G.; Móczó, J.; Pukánszky, B. *Polym. Adv. Technol.* **2006,** *17*, 967.
4. Espert, A.; Camacho, W.; Karlson, S. *J. Appl. Polym. Sci.* **2003,** *89*, 2353.
5. Bullions, T. A.; Gillespie, R. A.; Price-O'Brien, J.; Loos, A. C. *J. Appl. Polym. Sci.* **2004,** *92*, 3771.
6. Dányádi, L.; Jankecska, T.; Szabó, Z.; Nagy, G.; Móczó, J.; Pukánszky, B. *Compos. Sci. Technol.* **2007,** *67*, 2838.
7. Yang, H.; Kim, H.; Park, H.; Lee, B.; Hwang, T. *Compos. Struct.* **2007,** *77*, 45.
8. Bledzki, A. K.; Mamun, A. A.; Volk, J. *Compos. A* **2010,** *41*, 480.
9. Le Digabel, F.; Boquillon, N.; Dole, P.; Monties, B.; Averous, L. *J. Appl. Polym. Sci.* **2004,** *93*, 428.
10. Luz, S.; Goncalves, A.; Delarcojr, A. *Compos. A* **2007,** *38*, 1455.
11. Renner, K.; Móczó, J.; Suba, P.; Pukánszky, B. *Compos. Sci. Technol.* **2010,** *70*, 1141.
12. Panthapulakkal, S.; Sain, M. *Compos. A* **2007,** *38*, 1445.
13. Sui, G.; Fuqua, M. A.; Ulven, C. A.; Zhong, W. H. *Bioresource Technol.* **2009,** *100*, 1246.
14. Trejo-O'reilly, J. A.; Cavaillé, J. Y.; Paillet, M.; Gandini, A.; Herrera-Franco, P.; Cauich, J. *Polym. Compos.* **2000,** *21*, 65.
15. Kim, K. N.; Kimm, H.; Lee, J. W. *Polym. Eng. Sci.* **2001,** *41*, 1963.
16. Jang, L. W.; Kim, E. S.; Kim, H. S.; Yoon, J. S. *J. Appl. Polym. Sci.* **2005,** *98*, 1229.
17. Turcsányi, B.; Pukánszky, B.; Tüdõs, F. *J. Mater. Sci. Lett.* **1988,** *7*, 160.
18. Pukánszky, B. *Composites* **1990,** *21*, 255.
19. Sewda, K.; Maiti, S. N. *J. Appl. Polym. Sci.* **2009,** *112*, 1826.
20. Einstein, A. *Ann. Phys.* **1905,** *17*, 549.
21. Tavman, I. H. *J. Appl. Polym. Sci.* **1996,** *62*, 2161.
22. Kerner, E. H. *Proc. Phys. Soc. London Sect B.* **1956,** *69*, 808.
23. Counto, U. *J. Mag. Concr. Res.* **1964,** *16*, 129.